THE COSMIC EXPLORER GRAVITATIONAL WAVE OBSERVATORY

Technical Note	**CE-T2400011-v2**	2024/06/28

Higher-order mode scattering power loss due to spherical aberration

Liu Tao[a], Sagar Gupta[a], Paul Fulda[a]
[a] *University of Florida,*

This is an internal working
note of the COSMIC EXPLORER project.

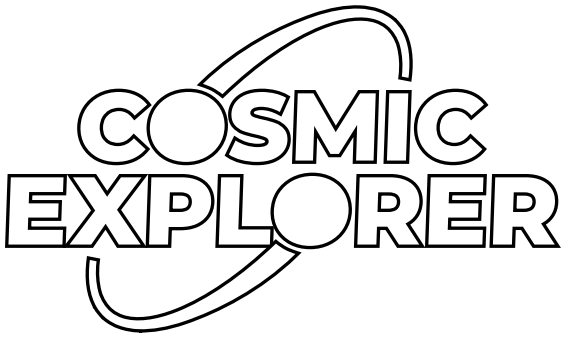

http://www.cosmicexplorer.org/

Introduction

A paraboloid perfectly describes the wavefront of the Gaussian laser beam, which slightly differs from the spherical surfaces of the mirrors used in the current gravitational wave (GW) detectors. The surface height difference, or error, from approximating the paraboloidal wavefront of the Gaussian beam with spherical mirror surface reflectors, or the spherical aberration, causes slight deviation to the laser beam wavefront upon reflection and produces losses. The paraboloid can be well approximated by a sphere with the same curvature, especially when near the center of the curved optics. However, as the beam gets larger, as is the case for next-generation GW detectors such as Cosmic Explorer, the beam wavefront error introduced by using spherical mirrors becomes non-negligible.

In this technical note, we interpret this phase front distortion from the spherical aberration in terms of higher-order mode (HOM) scattering through both analytical derivation and FINESSE simulation. We will demonstrate how the result gives us guidance in choosing the beam size on curved mirrors to limit the power scattering loss through spherical aberration. We will also consider such effects when the beam is slightly off-centered on the spherical mirror, and when we have a non-normal incidence beam on the curved mirror with an arbitrary angle of incidence.

Here we briefly summarize the results. For a beam perfectly centered on a spherical mirror with a normal incidence, the spherical aberration can be described in terms of HOM scattering into the 4th-order $\mathrm{HG}_{4,0}$, $\mathrm{HG}_{0,4}$, and $\mathrm{HG}_{2,2}$ modes, after a re-optimization of the HG mode basis procedure for better mode matching that minimizes the scattered second-order modes. The amplitudes of the 4th-order modes are characterized by the common HOM coefficient $\frac{kw^4}{32R^3}$, with additional scaling factors of $\sqrt{6}$, $\sqrt{6}$, and 2 for the $\mathrm{HG}_{4,0}$, $\mathrm{HG}_{0,4}$, and $\mathrm{HG}_{2,2}$ modes respectively. Adding all the contributions, the *total* power loss scattered into the 4th-order modes, due to spherical aberration, is $\frac{k^2w^8}{64R^6}$. One needs to keep the beam size reasonably small on the curved mirror to constrain the HOM scattering power loss to a given requirement.

The incident beam off-centered on the spherical mirror by a causes additional first-order mode scattering, which can be counteracted by tilting the curved mirror accordingly by $-\frac{a}{R}$. The remaining 4th-order mode scatterings from the spherical aberration in the deliberately tilted HG mode basis do not have a significant difference, compared against the HOM scatterings for a perfectly centered beam.

For an incident Gaussian beam with a non-normal angle of incidence θ, it results in changes to the surface height error as well as the beam transverse dimension. The amount of 4th order mode scattering is increased by a factor of $\frac{1}{(\cos\theta)^{n+1}}$ in the region with a reasonably small beam size, with n being the mode index in the same direction as the angle of incidence. For instance, for a beam incident with an angle of incidence θ in the $x-z$ plane, n is the mode index of the x component of the corresponding HG mode, i.e. $n = 4, 2, 0$ for the $\mathrm{HG}_{4,0}$, $\mathrm{HG}_{0,4}$, and $\mathrm{HG}_{2,2}$ modes respectively.

Analytical Derivation on Higher-order Hermite-Gauss Mode Scattering

The general expression for an HG mode is separable in the x and y direction

$$\mathcal{U}_{nm}(x,y,z) = \mathcal{U}_n(x,z)\mathcal{U}_m(y,z) \tag{1}$$

with

$$\begin{aligned}\mathcal{U}_n(x,y,z) = &\left(\frac{2}{\pi}\right)^{1/4}\left(\frac{\exp(i(2n+1)\Psi(z))}{2^n n! w(z)}\right)^{1/2} \\ &\times H_n\left(\frac{\sqrt{2}x}{w(z)}\right)\exp\left(-i\frac{kx^2}{2R_c(z)} - \frac{x^2}{w^2(z)}\right)\end{aligned} \tag{2}$$

We use the following properties of Hermite polynomials $H_n\left(\frac{\sqrt{2}x}{w(z)}\right)$ [1]

$$2\frac{\sqrt{2}x}{w(z)}H_n = H_{n+1} + 2nH_{n-1} \tag{3}$$

The beam wavefront is described by a paraboloid, with the curvature at the center equal to $R_c(z)$. Using spherical mirrors in interferometers, since it does not completely match the paraboloidal wavefront, the spherical aberration introduced can be characterized by the mirror surface figure height error

$$\Delta z = \underbrace{R - R\sqrt{1 - \frac{x^2+y^2}{R^2}}}_{\text{Sphere}} - \underbrace{\frac{x^2+y^2}{2R}}_{\text{paraboloid}} \approx \frac{(x^2+y^2)^2}{8R^3} \tag{4}$$

which is the surface height difference between the beam wavefront and the surface of the spherical mirror. In the region where the average beam size, characterized by x^2+y^2 in the transverse field amplitude, is much smaller than the mirror's radius of curvature R, one can also expand the surface height error Δz to the leading order as above.

The beam picks up an extra phase that is proportional to the surface height difference

$$\delta\phi = k \cdot 2\Delta z \tag{5}$$

where the factor of 2 comes from reflecting from the mirror. $k = \frac{2\pi}{\lambda}$ is the wavenumber. For an incident Gaussian beam with its amplitude described by $\mathcal{U}_{00}(x,y,z)$, the effect of the beam wavefront error $\delta\phi$ from spherical aberration can be expanded to the first-order

$$\mathcal{U}_{00}(x,y,z)\cdot e^{i\delta\phi} \approx \mathcal{U}_{00}(x,y,z)\,(1+i\delta\phi) = \mathcal{U}_{00}(x,y,z) + 2ik\,\mathcal{U}_{00}(x,y,z)\Delta z \tag{6}$$

The effect of the phase front distortion $\delta\phi$ can be described by the second term up to the leading contribution. Expanding the surface height error in Equation 4, and using the

properties of the Hermite polynomial in Equation 3 repeatedly, we can assemble the terms and write the leading contribution of the spherical aberration in terms of HOM scattering

$$\begin{aligned}\mathrm{HG}_{0,0}\cdot e^{i\delta\phi} \Longrightarrow \mathrm{HG}_{0,0} + i\frac{kw^4}{32R^3}\Big(&\sqrt{6}\times\mathrm{HG}_{4,0}\cdot e^{-4i\Psi} + \sqrt{6}\times\mathrm{HG}_{0,4}\cdot e^{-4i\Psi} + 2\times\mathrm{HG}_{2,2}\cdot e^{-4i\Psi}\\ &+ 4\sqrt{2}\times\mathrm{HG}_{2,0}\cdot e^{-2i\Psi} + 4\sqrt{2}\times\mathrm{HG}_{0,2}\cdot e^{-2i\Psi} + 4\times\mathrm{HG}_{0,0}\Big)\end{aligned} \tag{7}$$

The effect of spherical aberration through wavefront distortion on a reflecting Gaussian beam $\mathrm{HG}_{0,0}$ can be described in terms of mode scattering into the fourth-order modes $\mathrm{HG}_{0,4}$, $\mathrm{HG}_{0,4}$, and $\mathrm{HG}_{2,2}$, and into the second-order modes $\mathrm{HG}_{0,2}$ and $\mathrm{HG}_{2,0}$. The common amplitude coefficient of the HOM scattering is described by

$$\text{HOM Coefficient} = \frac{kw^4}{32R^3} \tag{8}$$

For instance, for the PR3 mirror in aLIGO, the beam size is roughly 0.054 m, and the radius of curvature (RoC) of PR3 is 36 m. The HOM amplitude for this case is $3.4\cdot10^{-5}$. The power loss scattered away for the HOMs would be the square of the amplitude. The *total* power scattered into the fourth-order modes are

$$\text{4th-order Mode Power Loss} = \frac{k^2w^8}{64R^6} \tag{9}$$

For the PR3 mirror in aLIGO with the nominal beam size, the 4th-order mode power scattering loss is of order 10^{-8}.

Finesse Simulation on Spherical Aberration

We have also looked at the effect of spherical aberration in terms of the 4th-order mode scattering in FINESSE. In particular, we consider a curved mirror with a RoC of 36 m. The Gaussian beam incident on the curved mirror forms a waist at the mirror location, with a nominal waist size of 0.054 m. The mirror surface figure map that characterizes the surface height error from spherical aberration is applied to the curved mirror, and the amount of HOM scattering is calculated in the reflection, as the beam size on the curved mirror increases.

The mirror maps that correspond to a perfectly centered beam, a slightly off-centered beam, as well as a non-normal incident beam with an arbitrary angle of incidence have been investigated. The effects of such mirror maps on the HOM scattering and the resulting power scattered losses have been studied.

Centered and Off-centered Beams

For a beam perfectly centered on the spherical mirror, as we have analytically studied earlier, the mirror height error can be described by Equation 4. The mirror height error as a function

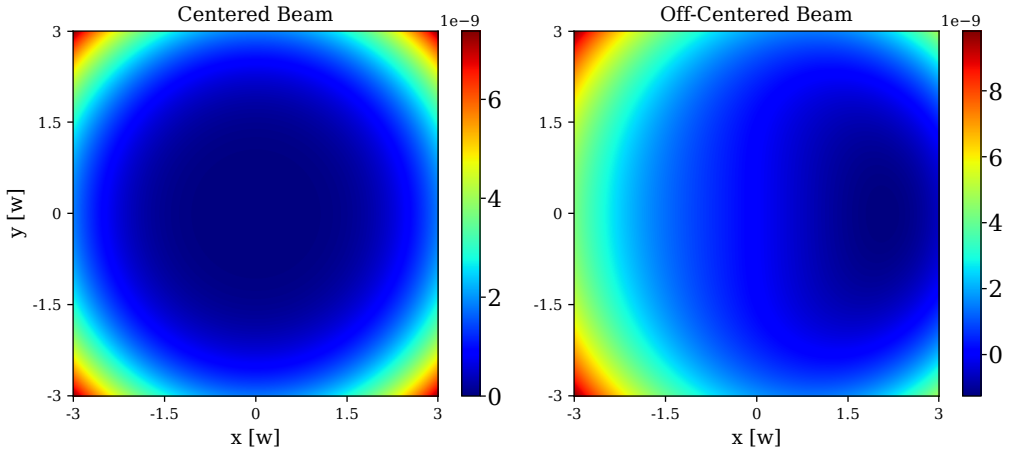

Figure 1: Phase map images that characterize the surface height error from spherical aberration. Left: the beam is perfectly centered on the spherical mirror; Right: the beam is slightly offset from the mirror center along the x direction.

of the transverse coordinates x and y can be presented in terms of two-dimensional mirror maps. An example of such a spherical aberration mirror map is shown on the left panel of Figure 1, in the region of $[-3w, 3w]$ with w being the nominal waist size. The surface height error is of order nanometers, which is small enough compared against the wavelength of the laser. It can be treated as small perturbations and expanded in the HG mode basis in FINESSE. The mirror maps are applied to the curved mirror in FINESSE and the result HOM scattering is calculated.

The HOM scattering into the 2nd order modes and the 4th order modes for a perfectly centered beam is shown in Figure 2. On the left panel, the HOMs are represented in the original Gaussian beam basis, in units of the HOM coefficient $\frac{kw^4}{32R^3}$ in Equation 8. The FINESSE result matches with the analytical result in Equation 7, when the beam size on the curved mirror PR3 is relatively small. As the beam gets large, the HOM coefficient gets large as well, as shown in the bottom panel in Figure 2. The resulting HOM scattering contents start to deviate from the analytical results as the non-leading contributions get more and more significant.

The HOM scattering into the 2nd order $\mathrm{HG}_{2,0}$ mode and $\mathrm{HG}_{0,2}$ mode indicates the original Gaussian beam basis is not the best basis for describing the disturbed beam. Instead, one should re-optimize the reflected beam basis with better mode matching that eliminates the scattered second-order mode contents. The result scattering into the 4th order $\mathrm{HG}_{0,4}$, $\mathrm{HG}_{4,0}$, and $\mathrm{HG}_{2,2}$ modes in the new optimized HG mode basis are shown on the right panel of Figure 2. The second-order mode scattering is minimized to a scale of less than one part per billion. This however does not cause a significant difference in the 4th-order mode scattering, since they are still well described by the HOM coefficients with the predicted scaling factors, indicating we can safely ignore the second-order scattered mode contents.

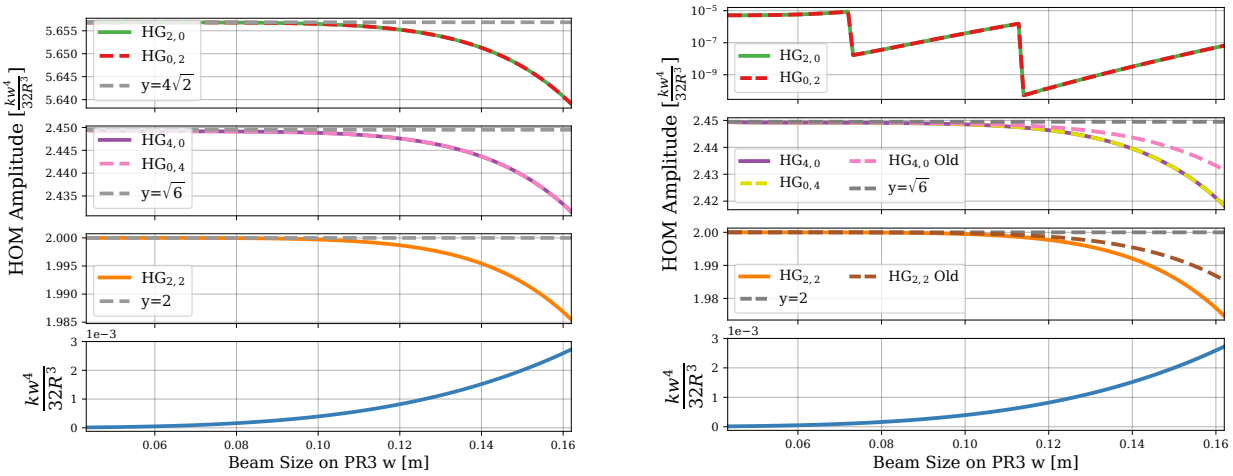

(a) HOM scattering to the second-order and the fourth-order modes in the original Gaussian beam basis

(b) HOM scattering in the re-optimized HG mode basis with better mode matching. The second-order modes are minimized

Figure 2: FINESSE simulation result on the higher-order mode scattering due to the spherical aberration for a perfectly centered beam, through applying mirror maps shown on the left panel of Figure 1 to curved mirror with radius of curvature equals to 36 m.

In the case of beam off-centering, say along the x direction by a, there is an additional significant scattering into the first-order $\mathrm{HG}_{1,0}$ mode

$$\mathrm{HG}_{1,0} \text{ mode from beam off-centering: } \frac{kaw}{R} \tag{10}$$

where w is the beam size, and R is the radius of curvature of the curved mirror. This also causes significant changes to the 4th-order scattered modes $\mathrm{HG}_{4,0}$ and $\mathrm{HG}_{2,2}$, and not so much for the $\mathrm{HG}_{0,4}$ mode, since only the x component of the HG modes would get affected. For instance, the resulting HOM scatterings for an off-centered input beam with increasing offsets for the nominal beam size case are shown on the left panel of Figure 3(a).

For a beam off-centered from a spherical mirror by a, one can tilt the mirror accordingly by $-a/R$ in radians to counteract the effect of beam off-centering. The result of the additional first-order mode and the 4th-order modes scattering are shown on the right panel of Figure 3(a). The scattering into the additional $\mathrm{HG}_{1,0}$ mode is minimized in the new deliberately tilted HG mode basis, and the 4th-order modes are back to the original case with the same scaling factors as with perfect beam centering.

Figure 3(b) shows the 4th-order mode scattering in the tilted mirror basis with increasing beam size. The HOM scattering is close to the original case with perfect beam centering, indicating the effect of small beam off-centering causes no significant difference to the 4th-order mode scattering, in the new basis with the mirror tilted accordingly.

Normal and non-normal Incident Beam

Here we look at the effect of a non-normal incident beam on the 4th-order mode scattering caused by spherical aberration. Figure 4 illustrates the effect of such non-normal beam

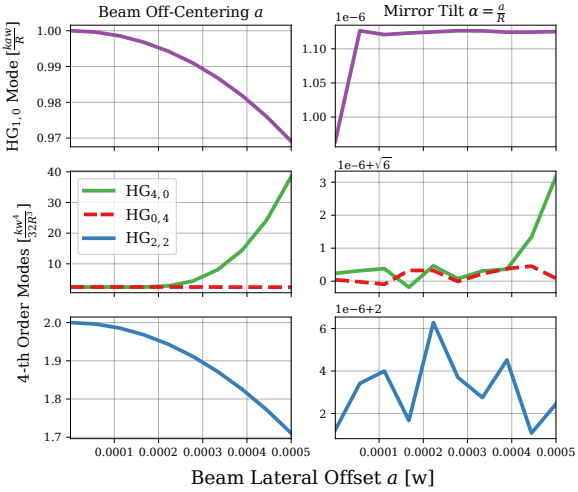

(a) The first-order and fourth-order mode scattering for an off-centered incident beam. Left: beam off-centering results in additional first-order mode scattering; Right: the effect can be counteracted in the titled HG mode basis.

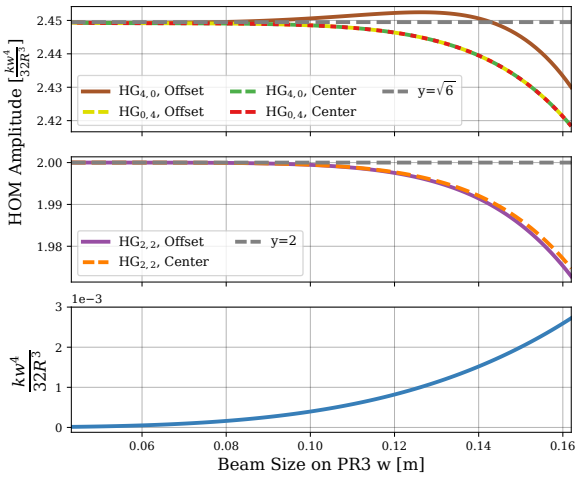

(b) The remaining fourth-order mode scattering in the new tilted HG mode basis that minimizes the additional scattered first-order mode, with increasing beam size on the curved mirror.

Figure 3: FINESSE simulation result on the higher-order mode scattering due to the spherical aberration for an off-centered incident beam, through applying mirror maps shown on the right panel of Figure 1 to curved mirror with radius of curvature equals to 36 m.

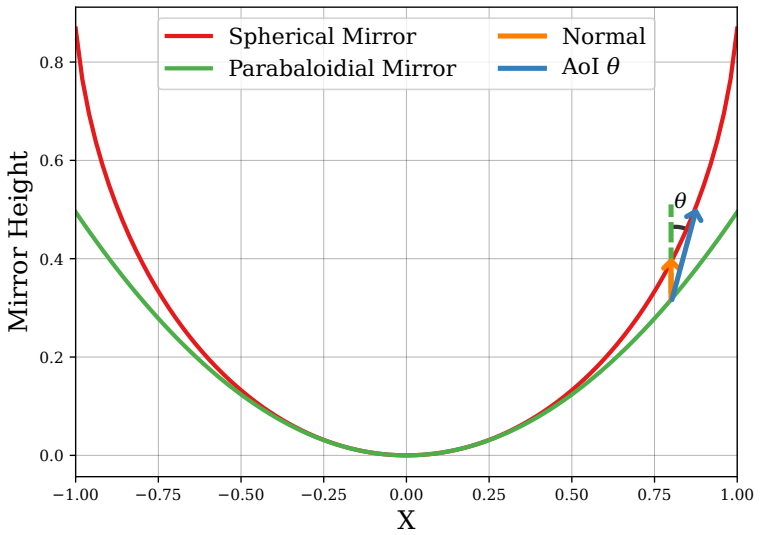

Figure 4: Illustration of the effect of beam non-normal incidence on the surface error. The surface error is characterized by the orange arrow for a normal incident beam, and by the blue arrow for a non-normal incident beam with an angle of incidence of θ.

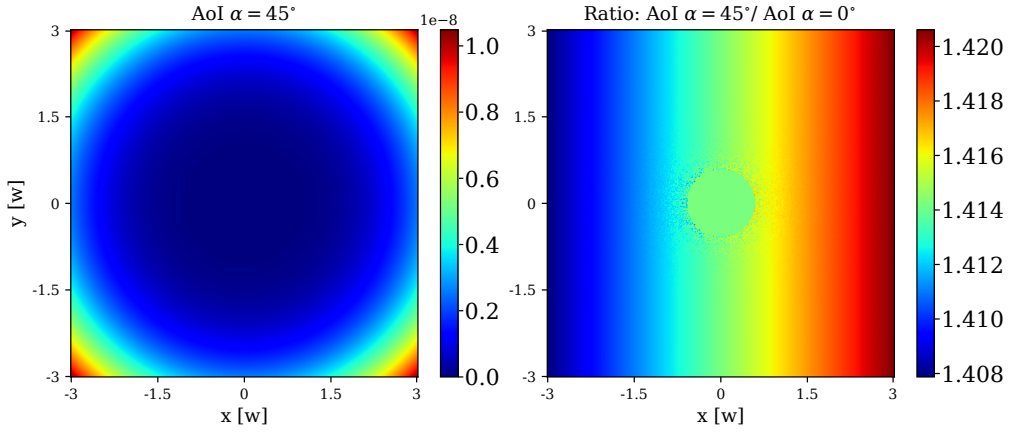

Figure 5: Phase maps that characterize the surface error from spherical aberration. Left: the beam is incident on the spherical mirror with $45°$ angle of incidence; Right: The ratio of the phase map with $45°$ angle of incidence to the phase map with normal incidence.

incidence on the mirror surface height difference between the paraboloidal wavefront and the spherical mirror, for a beam incident in the $x-z$ plane. The mirror surface height error is illustrated by the orange arrow for a normal incident beam, and by the blue arrow for a non-normal incident beam with an angle of incidence of θ.

This causes two effects on the mirror maps. The mirror surface height becomes different in the whole map region due to the angle of incidence. One can see the ratio of them becomes $1/\cos\theta$ when the x location is significantly close to the mirror center so the arrow tops are close to the same level. The angle of incidence also causes the width in the x dimension to shrink as seen by the incident beam. The changes in the mirror maps effectively cause the higher-order mode scattering to change.

Figure 5 shows the mirror surface figure map for a $45°$ incident beam on the left panel, and the right panel shows the ratio of the surface height error mirror maps for the $45°$ incident beam to the case of normal incident beam. We see the ratio is close to $1/\cos(45°) = \sqrt{2}$ in the region of $[-3w, 3w]$, with w being the nominal waist size, as expected.

The resulting HOM scatterings due to the phase maps corresponding to the non-normal angle of incidence are shown in Figure 6. We have again switched to a new optimized HG mode basis for the scattered HOMs so the second-order modes are minimized as a result of the mode-matching optimization. The scatterings into the 4th order $\mathrm{HG}_{4,0}$, $\mathrm{HG}_{0,4}$, and $\mathrm{HG}_{2,2}$ modes are again described in terms of the common HOM coefficient $\frac{kw^4}{32R^3}$.

The effect of a non-normal angle of incidence on the spherical aberration can be described by an increase in the 4th-order mode scattering by a factor of $\frac{1}{(\cos\theta)^{n+1}}$, where n is the mode index for the x component of the corresponding 4th-order mode. This is because the new X axis dimension seen by the beam is shrunk by roughly a factor of $\frac{1}{\cos\theta}$ when the beam size is reasonably small. Each mode order in x results in an increment of the HG mode amplitude by the same $\frac{1}{\cos\theta}$ factor in the new X axis. The additional increment factor $\frac{1}{\cos\theta}$ for all HOM scattering is due to the increment of surface height error in the mirror maps, as shown in Figure 5.

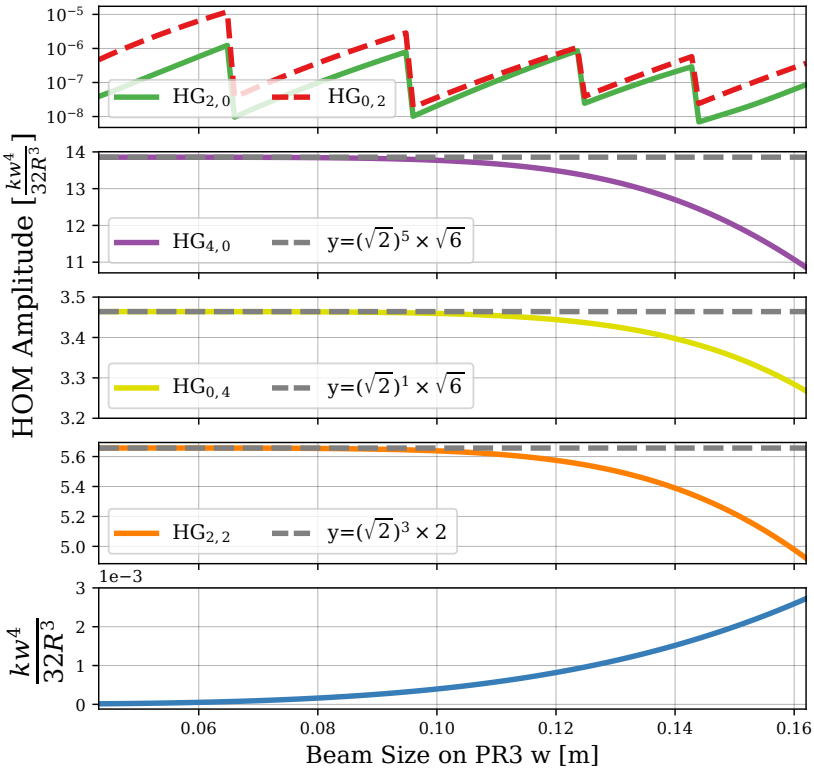

Figure 6: The higher-order mode scattering into the 4th-order modes $\mathrm{HG}_{4,0}$, $\mathrm{HG}_{0,4}$, and $\mathrm{HG}_{2,2}$ modes for a non-normal incident beam with $45°$ angle of incidence.

For instance, for the $\mathrm{HG}_{2,2}$ mode scattering from a $45°$ incident beam, the scattered coefficient is increased by a factor of $\sqrt{2}^{2+1} = \sqrt{2}^{3}$, compared against the original normal incidence case, as shown in Figure 6. The $\mathrm{HG}_{4,0}$ and $\mathrm{HG}_{0,4}$ mode scatterings are affected differently, due to the different mode index in the x direction. The $\mathrm{HG}_{4,0}$ scattered mode coefficient is increased by a factor of $\sqrt{2}^{4+1} = \sqrt{2}^{5}$, whereas the $\mathrm{HG}_{0,4}$ mode coefficient is only increased by a factor of $\sqrt{2}^{0+1} = \sqrt{2}$.

0.1 Aberration due to a lens

Much of what is discussed above about curved mirrors can be applied to lenses as well with a few modifications. The phase map in eq.5 is modified as

$$\delta\phi = k \cdot (n-1) \cdot \Delta z \tag{11}$$

where n is the refractive index of the lens. We perform the simulation using the resonant beam parameter in a 40km long FP cavity to be used in CE with the radius of curvatures of the test masses being 29870m each and get the power scattered into the higher order modes as a function of the outer radius of curvature. The results are shown in Figure 7. We only plot certain higher order modes because of the quadratic nature of Δz (same as the mirror case). Taking into account the loss budget for CE, a radius of curvature as small as

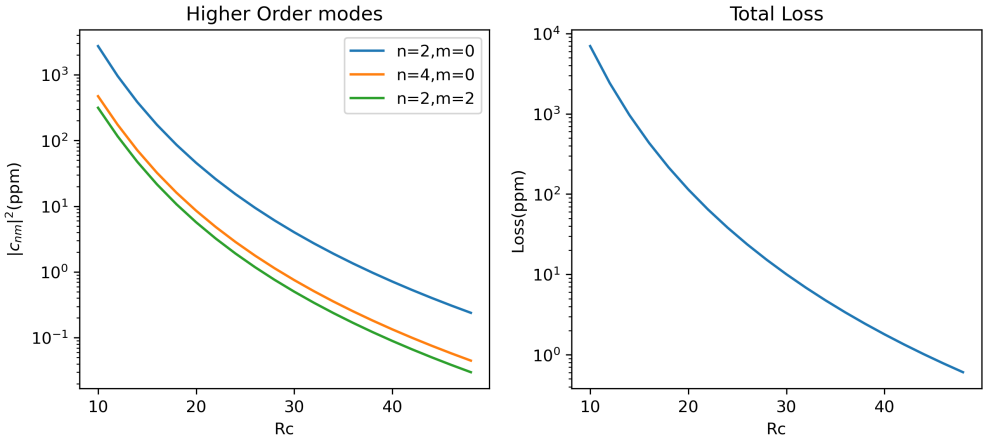

Figure 7: Scattering into Higher Order HG modes due to Spherical Aberration through ITM lens. Left: Power scattered into specific Higher Order HG modes. Right: Total loss due to scattering.

15m might be possible, however effects of mode healing/harming inside the recycling cavities needs to be studied to gauge how small the radius of curvature can be made.

References

[1] Liu Tao, Jessica Kelley-Derzon, Anna C. Green, and Paul Fulda. Power coupling losses for misaligned and mode-mismatched higher-order hermite–gauss modes. *Opt. Lett.*, 46(11):2694–2697, Jun 2021.